Cerebral Cortex Advance Access published October 9, 2013

Cerebral Cortex
doi:10.1093/cercor/bht261

Capturing with EEG the Neural Entrainment and Coupling Underlying Sensorimotor Synchronization to the Beat

Sylvie Nozaradan[1,2], Younes Zerouali[3], Isabelle Peretz[2] and André Mouraux[1]

[1]Institute of Neuroscience (IONS), Université catholique de Louvain (UCL), Belgium, [2]International Laboratory for Brain, Music and Sound Research (BRAMS), Université de Montréal, Canada and [3]Ecole de Technologie Supérieure, Université de Montréal, Canada

Address correspondence to Dr André Mouraux, Institute of Neurosciences, Université catholique de Louvain, 53, Avenue Mounier – UCL 53.75, B-1200 Bruxelles, Belgium. Email: andre.mouraux@uclouvain.be

Synchronizing movements with rhythmic inputs requires tight coupling of sensory and motor neural processes. Here, using a novel approach based on the recording of steady-state-evoked potentials (SS-EPs), we examine how distant brain areas supporting these processes coordinate their dynamics. The electroencephalogram was recorded while subjects listened to a 2.4-Hz auditory beat and tapped their hand on every second beat. When subjects tapped to the beat, the EEG was characterized by a 2.4-Hz SS-EP compatible with beat-related entrainment and a 1.2-Hz SS-EP compatible with movement-related entrainment, based on the results of source analysis. Most importantly, when compared with passive listening of the beat, we found evidence suggesting an interaction between sensory- and motor-related activities when subjects tapped to the beat, in the form of 1) additional SS-EP appearing at 3.6 Hz, compatible with a nonlinear product of sensorimotor integration; 2) phase coupling of beat- and movement-related activities; and 3) selective enhancement of beat-related activities over the hemisphere contralateral to the tapping, suggesting a top-down effect of movement-related activities on auditory beat processing. Taken together, our results are compatible with the view that rhythmic sensorimotor synchronization is supported by a dynamic coupling of sensory and motor related activities.

Keywords: EEG, music cognition, neuronal entrainment, rhythm perception, sensorimotor synchronization, steady-state-evoked potentials

Introduction

Synchronizing movements to external inputs is best observed with music (London 2004; Repp 2005; Janata et al. 2012). Perception of beat in music refers to the spontaneous human ability to perceive periodicities from sequences of sounds (London 2004). The regular temporal structure of beats is thought to facilitate movement synchronization on musical rhythms. Indeed, one of the fascinating aspects of beat perception is its strong relationship with movement (Phillips-Silver and Trainor 2005; Madison 2006; Grahn and Brett 2007; Chen et al. 2008; Phillips-Silver et al. 2010; Janata et al. 2012; Teki et al. 2011). First, music spontaneously entrains humans to move (vanNoorden and Moelants 1999; Madison 2006; Phillips-Silver et al. 2010; Janata et al. 2012). Second, it has been shown that movement influences the perception of musical rhythms (Phillips-Silver and Trainor 2005, 2007). Third, functional neuroimaging studies have shown that motor cortical areas are activated when listening to rhythmic sequences (Grahn and Brett 2007; Chen et al. 2008; Teki et al. 2011).

How distant brain areas involved in sensorimotor synchronization are able to coordinate their dynamics remains, at present, largely unknown. Two main theories have been proposed (Pressing 1998; Repp 2005). The information-processing theory considers responses to the beat as a succession of discrete events and proposes that sensorimotor synchronization is achieved through error correction mechanisms occurring from one event to the other (Vorberg and Wing 1995; Pressing 1998; Praamstra et al. 2003). Contrasting with this view, the dynamic systems theory postulates that sensorimotor synchronization results from a dynamic and continuous coupling of sensory and motor oscillators (Beek et al. 2002; Hogan and Sternad 2007). This second hypothesis is in line with the hypothesis that beat perception is represented in the human brain as a dynamic prediction or attending process, in which the periodic temporal structure of the auditory beat entrains the listener's attention, leading to a periodic modulation of expectancy as a function of time (Jones and Boltz 1989; Large and Jones 1999). Building on this view, the resonance theory for beat perception (Large and Kolen 1994; Large 2008) proposes that the perception of periodicities in music emerges from the entrainment of neural populations resonating at the frequency of the beat. Recently, we provided direct evidence of such neural entrainment to musical beats in humans using electroencephalography (EEG) (Nozaradan et al. 2011; Nozaradan et al. 2012a, 2012b). Specifically, we showed that an auditory beat elicits a periodic neural response at the exact frequency of the beat. This oscillatory activity, frequency-locked to the beat and captured in the EEG signal in the form of a steady-state evoked potential (SS-EP) (Regan 1989), was hypothesized to reflect the neural entrainment underlying beat perception.

Here, we used this novel approach to explore the neural dynamics supporting sensorimotor synchronization to the beat, that is, the performance of overt movements paced on the beat. Specifically, we hypothesized that sensorimotor synchronization to the beat is supported in the human brain by 2 distinct neural entrainments: a neural entrainment at the frequency of the beat which would underlie beat processing (Large 2008; Nozaradan et al. 2011) and a distinct neural entrainment at the frequency of the movement which would underlie the production of synchronized movements (Gerloff et al. 1997, 1998; Kopp et al. 2000; Daffertshofer et al. 2005; Kourtis et al. 2008; Bourguignon et al. 2011). Furthermore, we hypothesized that SS-EP frequency tagging would allow us to disentangle beat- and movement-related EEG responses based on their respective frequencies and, therefore, we examined whether this approach could be used to characterize the sensorimotor coupling hypothesized to support motor synchronization to an auditory beat.

Materials and Methods

Subjects

Eight healthy volunteers (3 females, all right-handed, mean age 27 ± 4 years, aged between 22 and 36) took part in the study after providing written informed consent. They all had musical experience, either in performance (3 subjects with 15–25 years of practice) or as amateur listeners or dancers. None had prior experience with the tapping task used in the present study. They had no history of hearing, neurological or psychiatric disorder, and were not taking any drug at the time of the experiment. The study was approved by the local Ethics Committee.

Auditory Stimulation

Each auditory stimulus lasted 33 s. The stimulus consisted of a 333.33-Hz pure tone in which a beat was introduced by modulating the amplitude of the tone with a 2.4-Hz periodicity (i.e., 144 beats per minute), using an asymmetrical Hanning envelope (12 ms rise time and 404 ms fall time, amplitude modulation between 0.25 and 1). A 2.4-Hz periodicity was chosen because 1) this tempo lies within the ecological range of tempo perception and production (Drake and Botte 1993), 2) we previously showed that this beat frequency elicits a measurable beat-related SS-EP in the human EEG (Nozaradan et al. 2011), and 3) pilot experiments showed that subjects are comfortable in tapping on every second beat using this beat frequency. The auditory stimuli were generated using the PsychToolbox extensions (Brainard 1997) running under Matlab 6.5 (The MathWork, USA), and presented binaurally through electromagnetically shielded insert earphones at a comfortable hearing level (ER 3A, Etymotic Research, Elk Grove Village, IL, USA).

Experimental Conditions

Subjects were comfortably seated in a chair with their head resting on a support. They were instructed to relax, avoid any unnecessary head or body movement and keep their eyes fixated on a point displayed on a computer screen in front of them. Subjects were asked to perform 3 different tasks: a control auditory task, a right hand tapping task and a left hand tapping task, in 3 separate conditions (Fig. 1). The tapping task was performed using each hand to assess the hemispheric lateralization of EEG activities relative to the tapping hand. Each condition consisted of 6 trials during which the 33-s auditory stimulus was presented after a 3-s foreperiod. Stimulus presentation was self-paced. During the first condition, subjects performed the control auditory task. They were asked to listen carefully to the periodic sound in order to detect the occurrence of a very short (4 ms) sound interruption, inserted at a random position in 2 additional trials interspersed within the block. The subjects were instructed to report their detection at the end of each trial. This control task required a sustained level of attention, and thus ensured that attention was focused on the sound. The 2 trials containing a short interruption were excluded from further analyses. During the second condition, subjects performed the right hand tapping task. They were asked to perform tapping movements with their right hand, accurately paced on every second beat of the sequence, that is, at half the beat frequency ($f/2 = 1.2$ Hz). During the third condition, they performed the same task, this time using their left hand. Before the right and left hand tapping conditions, a short training session ensured that subjects understood the task. The subjects were asked to start their tapping as soon as they heard the first auditory beat of the stimulus, and to maintain their movement as synchronized as possible throughout the entire trial. The tapping was performed with small up and down movements of the hand starting from the wrist joint, maintaining the forearm and elbow fixed on an armrest cushion. When performing the tapping movement, the fingers of the tapping hand came transiently in contact with the armrest cushion. All subjects naturally synchronized their movement such that the occurrence of this contact coincided with the occurrence of the beat. Importantly, the contact with the armrest produced tactile feedback, but did not produce any auditory feedback, as the subjects were fitted with earphone inserts. The experimenter remained in the recording room at all times, to monitor compliance to these instructions.

EEG Recording

The EEG was recorded using 64 Ag-AgCl electrodes placed on the scalp according to the International 10/10 system (Waveguard64 cap, Cephalon A/S, Denmark). Vertical and horizontal eye movements were monitored using 4 additional electrodes placed on the outer canthus of each eye and on the inferior and superior areas of the left orbit. Electrode impedances were kept below 10 kΩ. The signals were amplified, low-pass filtered at 500 Hz, digitized using a sampling rate of 1000 Hz, and referenced to an average reference (64-channel high-speed amplifier, Advanced Neuro Technology, the Netherlands).

Hand Movement Recordings

Movements of the hand were measured using a 3-axis accelerometer attached to the hand dorsum (MMA7341L, Pololu Robotics and Electronics, USA). The signals generated by the accelerometer were digitized using 3 additional bipolar channels of the EEG system. Only

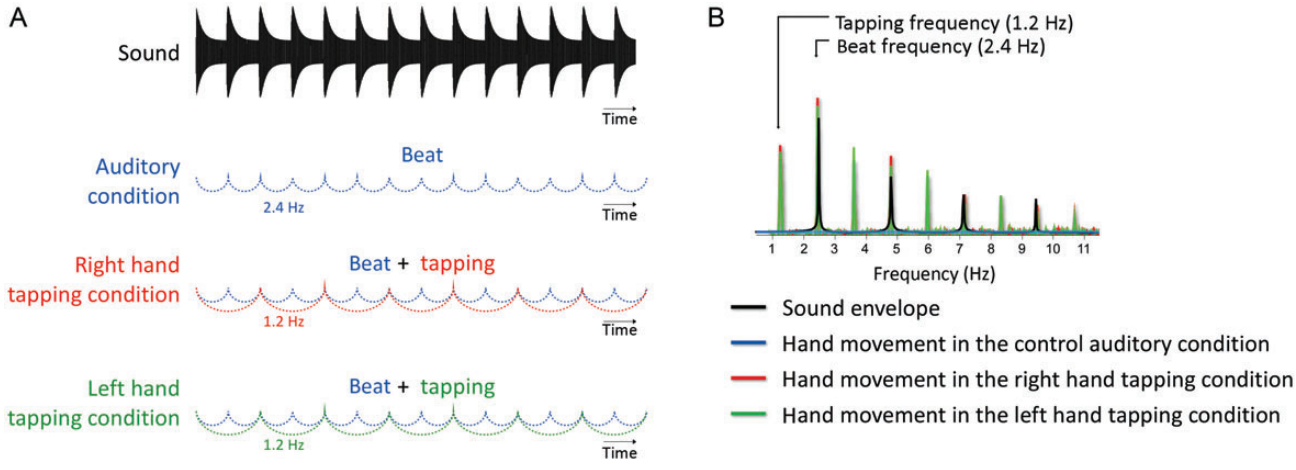

Figure 1. Experimental paradigm and hand movement signals. (*A*) The auditory stimulus consisted of a 33-s pure 333.33-Hz tone in which a beat was introduced by modulating the amplitude of the tone with a 2.4-Hz periodicity. The upper graph shows a 6 s excerpt of its sound envelope. In the control auditory condition, the participants were asked to listen to the sound, in order to detect the occasional occurrence of a short discontinuity. In the left and right hand tapping conditions, the participants were asked to perform a hand tapping movement paced on every second beat in the sequence (i.e., at 1.2 Hz, corresponding to half the frequency of the beat). (*B*) Frequency spectrum of the sound envelope (black) and the accelerometer signals recorded from the hand in the control auditory condition (blue), the right hand tapping condition (red), and the left hand tapping condition (green).

the vertical axis of the accelerometer signal was analyzed, as it sampled the greatest part of the accelerations related to the tapping movement.

Frequency-Domain Analysis

SS-EP Amplitude

Continuous EEG recordings were filtered using a 0.1-Hz high-pass Butterworth zero-phase filter to remove very slow drifts in the recorded signals. Epochs lasting 32 s were obtained by segmenting the recordings from +1 to +33 s relative to the onset of the auditory stimulus, thus yielding 6 epochs for each subject and condition. The EEG recorded during the first second of each epoch was removed 1) to discard the transient auditory evoked potentials related to the onset of the stimulus (Saupe et al. 2009; Nozaradan et al. 2011, 2012a, 2012b), 2) because SS-EPs require several cycles of stimulation to be steadily entrained (Regan 1989), and 3) because several repetitions of the beat are required to elicit a steady perception of beat (Repp 2005). These EEG processing steps were carried out using Analyzer 1.05 (Brain Products, Germany).

Artifacts produced by eye blinks or eye movements were removed from the EEG signal using a validated method based on an Independent Component Analysis (Jung et al. 2000), using the Runica algorithm (Bell and Sejnowski 1995; Makeig 2002). For each subject and condition, EEG epochs were averaged across trials. The time-domain averaging procedure was used to enhance the signal-to-noise ratio of beat- and movement-related EEG activities by attenuating the contribution of activities that were not strictly phase-locked across trials, that is, activities that are not phase-locked to the sound stimulus. The obtained average waveforms were then transformed in the frequency domain using a discrete Fourier transform (Frigo and Johnson 1998), yielding a frequency spectrum of signal amplitude (μV) ranging from 0 to 500 Hz with a frequency resolution of 0.031 Hz (Bach and Meigen 1999). These EEG processing steps were carried out using Letswave (Mouraux and Iannetti 2008), Matlab (The MathWorks, USA), and EEGLAB (http://sccn.ucsd.edu).

Within the obtained frequency spectra, signal amplitude may be expected to correspond to the sum of 1) EEG activity induced by the auditory beat and/or the hand movement task, referred as to beat- and movement-related SS-EPs and 2) unrelated residual background noise due, for example, to spontaneous EEG activity, muscle activity, or eye movements. Therefore, to obtain valid estimates of beat- and movement-related SS-EPs, the contribution of this noise was removed by subtracting, at each bin of the frequency spectra, the average amplitude measured at neighboring frequency bins (2 frequency bins ranging from −0.15 to −0.09 Hz and from + 0.09 to + 0.15 Hz relative to each frequency bin). The validity of this subtraction procedure relies on the assumption that, in the absence of an SS-EP, the signal amplitude at a given frequency bin should be similar to the signal amplitude of the mean of the surrounding frequency bins (Mouraux et al. 2011; Nozaradan et al. 2011, 2012a, 2012b). This subtraction procedure is important because the magnitude of the background noise is not equally distributed across scalp channels (Supplementary Material). Indeed, without this subtraction procedure, the scalp topographies of the elicited SS-EPs would reflect a combination of the scalp distribution of the SS-EP response and the scalp distribution of the background noise present at that frequency.

The magnitude of beat- and movement-related SS-EPs was then estimated by averaging the noise-subtracted amplitudes measured at the frequency bins centered over the expected 1.2-Hz movement-related SS-EP (bins ranging from 1.178 to 1.240 Hz) and the expected 2.4-Hz beat-related SS-EP (bins ranging from 2.356 to 2.418 Hz). This range of frequencies allowed accounting for possible spectral leakage due to the fact that the discrete Fourier transform did not estimate signal amplitude at the exact frequency of each SS-EP (Nozaradan et al. 2011, 2012a, 2012b). In the right and left hand tapping conditions, an additional SS-EP appeared at 3.6 Hz in the EEG frequency spectrum of all subjects (Fig. 2). The magnitude of this additional SS-EP was estimated by averaging the signal amplitude measured at the bins ranging from 3.562 to 3.624 Hz.

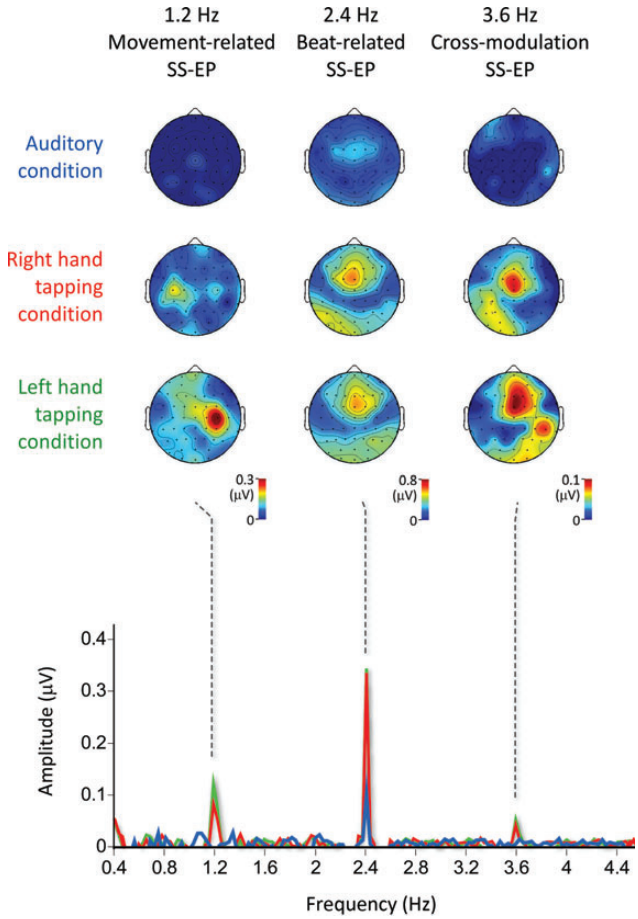

Figure 2. Group-level average frequency spectra (Hz) of the noise-subtracted EEG amplitude signals obtained in the control auditory condition (blue), the right hand tapping condition (red), and the left hand tapping condition (green), averaged across all scalp channels. In all conditions, the 2.4-Hz auditory beat elicited an SS-EP at 2.4 Hz. As shown in the corresponding topographical maps, this beat-related SS-EP was maximal over fronto-central electrodes. In the left and right hand-tapping conditions, the 1.2-Hz hand tapping movement was related to the appearance of an additional SS-EP at 1.2 Hz. As shown in the topographical maps, this movement-related SS-EP was maximal over the central electrodes contralateral to the moving hand. In these 2 conditions, an additional SS-EP emerged at 3.6 Hz, referred to as cross-modulation SS-EP, whose scalp topography showed patterns similar to both beat-related and movement-related SS-EPs topographies.

To exclude any electrode selection bias, the estimated magnitudes of the 1.2-, 2.4-, and 3.6-Hz SS-EPs were averaged across all scalp electrodes, for each condition and participant (Figs 2 and 3). A 1-sample *t*-test was then used to determine whether the average SS-EP amplitudes were significantly different from zero. Indeed, in the absence of an SS-EP, the average of the noise-subtracted signal amplitude may be expected to tend towards zero. Furthermore, a 1-way repeated-measures ANOVA was used to compare the magnitude of the SS-EPs recorded in each of the 3 experimental conditions (control, left hand tapping, right hand tapping). Degrees of freedom were corrected using the Greenhouse-Geisser correction for violations of sphericity. Size effects were expressed using the partial Eta-squared. When significant, post hoc pairwise comparisons were performed using paired-sampled *t*-tests. Significance level was set at $P < 0.05$. Finally, for each condition, topographical maps were computed by spherical interpolation for the 1.2-, 2.4-, and 3.6-Hz SS-EPs (Fig. 2).

Hand Tapping Movement

The accelerometer signals generated by the hand tapping movements were analyzed in the frequency domain using the same procedure

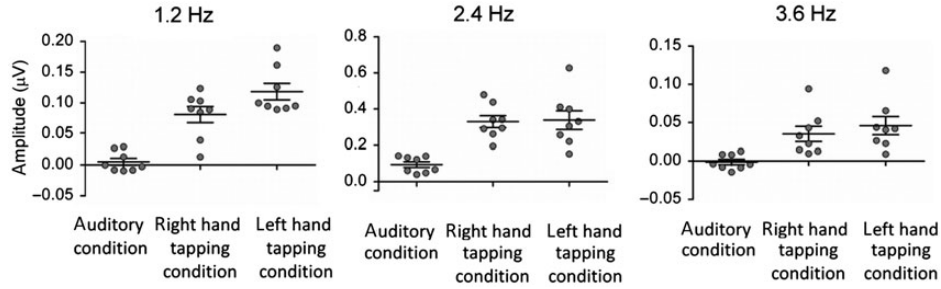

Figure 3. Amplitude of the 1.2-, 2.4-, and 3.6-Hz EEG activity in the control auditory condition, the right hand tapping condition and the left hand tapping condition. Dots represent individual noise-subtracted amplitude values obtained at each target frequency, averaged across all scalp electrodes. The whisker plots represent the group-level mean and standard error of the mean.

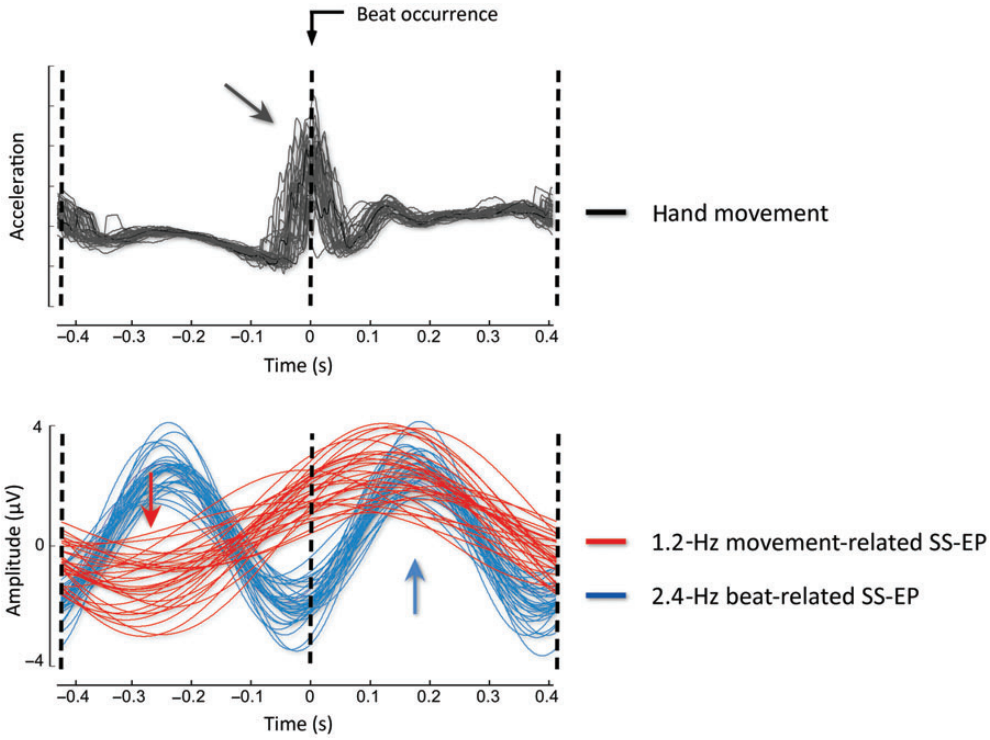

Figure 4. Time-domain analysis of the hand movement (vertical acceleration), the beat-related SS-EP and the movement-related SS-EP signals in 1 representative participant (right hand tapping condition). The upper graph represents the superimposed hand movement signals obtained for each tapping-movement cycle. The lower graph represents the superimposed beat-related (blue) and movement-related (red) EEG signals obtained after narrow-band filtering around 2.4 and 1.2 Hz, respectively (see Materials and Methods section for details). The dashed black lines represent the onset of the beat within these tapping-movement cycles. The trials are centered on the occurrence of the beats onto which the subjects synchronized their tapping. The colored arrows point to the relative latencies of the beat- and movement-related SS-EPs.

used to analyze the EEG signals. A 1-sample *t*-test was used to examine whether the noise-subtracted amplitude measured at 1.2 Hz in the tapping conditions was significantly different from zero. Indeed, in the absence of a periodic hand movement at 1.2 Hz, the average of the noise-subtracted signal amplitude may be expected to tend towards zero. Furthermore, a 1-sample *t*-test was used to compare the noise-subtracted amplitude at 1.2 Hz obtained across the 2 tapping conditions (right and left hand tapping).

Time-Domain Analysis

Time domain analyses were carried out to assess the phase coupling between beat-related and movement-related EEG activities, as well as the phase coupling between these activities and the hand tapping movement (Figs 4 and 5), as follows.

Hand Tapping Movement

The vertical acceleration signals recorded within each subject and tapping conditions were averaged across trials, to attenuate the contribution of unrelated signals not phase-locked to the sound stimulus. These average waveforms, lasting 33 s, were further segmented in epochs aligned to the occurrence of each beat onto which the subjects tapped, and extending from −0.416 to +0.416 s relative to the beat onset. Thus, these epochs expressed the across-trial average of the time course of the movement signal within each 1.2-Hz tapping-movement cycle (Fig. 4). The tapping latency relative to the beat occurrence was defined as the latency of maximum acceleration within each tapping-movement cycle (Figs 4 and 5). To assess the synchronization lag of each subject, a 1-sample *t*-test against zero was used to examine whether the mean relative tapping latencies were significantly different from zero in each of the 2 tapping conditions. Furthermore, a paired sample *t*-test was used to compare tapping latencies obtained in the left and right hand tapping conditions.

Beat-Related SS-EP

For each subject and condition, EEG oscillations corresponding to the beat-related SS-EP were extracted using a narrow band-pass FFT filter

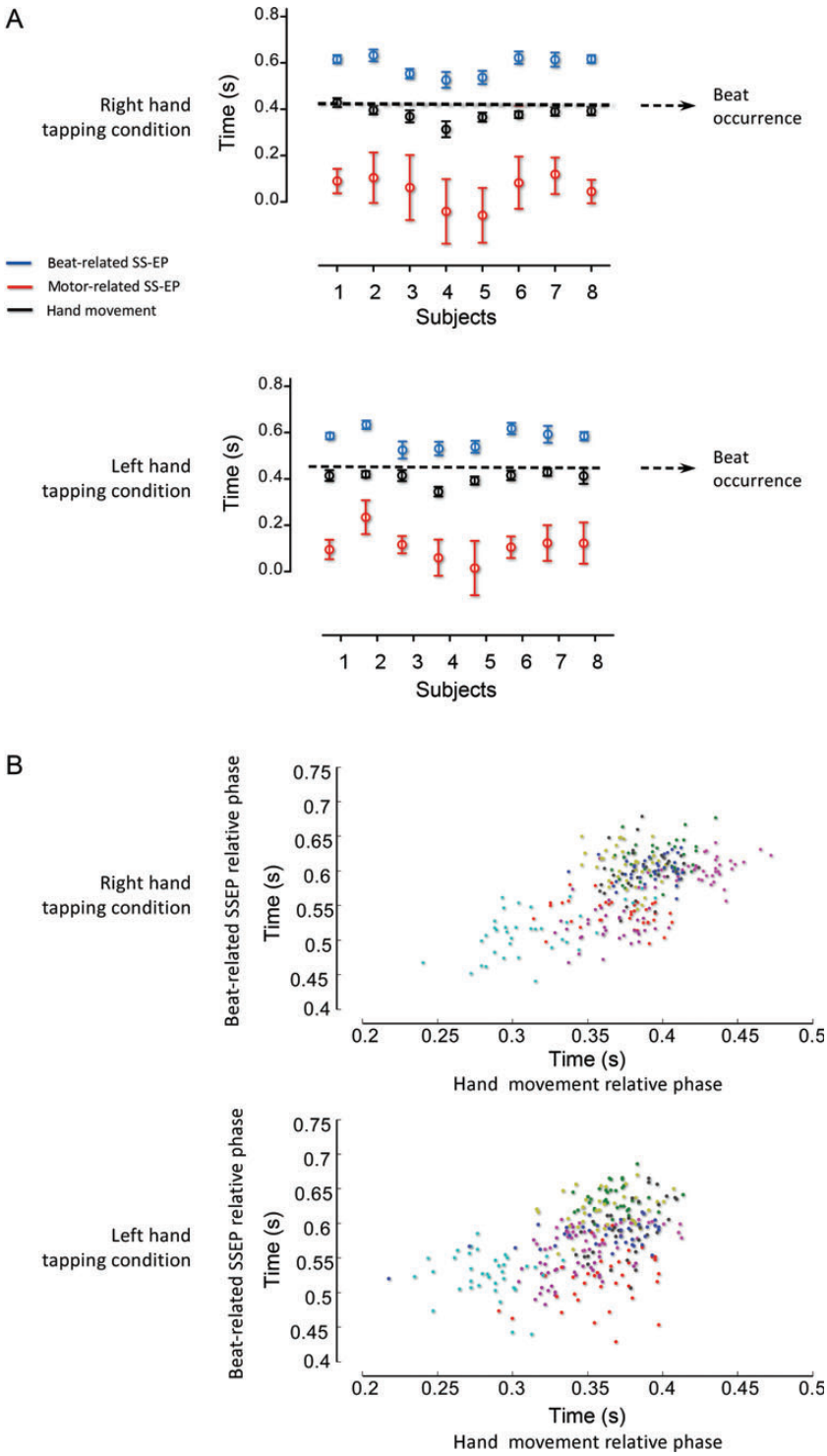

Figure 5. (*A*) Relative latencies of the hand tapping movement (black), the beat-related SS-EP (blue), and the movement-related SS-EP (red) estimated for each individual subject (1–8). The upper graph shows the results obtained in the right hand tapping condition whereas the lower graph shows the results obtained in the left hand tapping condition. The whisker plots represent the mean and standard deviation of the latencies obtained in each hand tapping cycle. The horizontal dashed line represents the actual occurrence of the beat to which subjects synchronized their tapping. (*B*) Scatter plot expressing the relative latencies of the beat-related SS-EP as a function of hand tapping movement in the right hand tapping condition (upper graph) and the left hand tapping condition (lower graph). Each dot represents a different hand tapping cycle. The different subjects are represented using different colors.

centered at 2.4 ± 0.4 Hz as width of the FFT window (Hanning function). The filtered signals were then averaged and segmented using the same procedure as for the accelerometer signals (Fig. 4). The electrode displaying the maximum amplitude at 2.4 Hz within the noise-subtracted frequency spectra was chosen as electrode of interest. This electrode selection criterion was used to maximize the signal-to-noise ratio of the analyzed signals and, thereby, reduce the contribution of residual noise when estimating phase coupling. Within each tapping

movement cycle, the relative latency of the beat-related SS-EP was arbitrarily defined as the latency of maximum amplitude of the oscillation following the occurrence of the beat (Figs 4 and 5). A repeated-measures ANOVA was then used to compare the mean relative latencies obtained in each condition (control, right hand tapping, and left hand tapping). When significant, post hoc pairwise comparisons were performed using paired-sampled *t*-tests.

Movement-Related SS-EP

The same procedure was used to extract EEG oscillations corresponding to the movement-related SS-EP, and to estimate their relative latencies in the right and left hand tapping conditions. The movement-related SS-EP was extracted using a band-pass filter centered at 1.2 ± 0.4 Hz. The electrode displaying the maximum amplitude at 2.4 Hz within the noise-subtracted frequency spectra was chosen as electrode of interest. The relative latency of the movement-related SS-EP was arbitrarily defined as the latency of maximum value of amplitude of the oscillation preceding the occurrence of the beat (Figs 4 and 5). A paired sample *t*-test was used to compare the mean relative latencies obtained in the left and right hand tapping conditions.

Phase Coupling

The relative latencies of the beat- and movement-related SS-EPs as well as that of the hand tapping movements were averaged across the left and right hand tapping conditions, as the values obtained for each of the 2 conditions were not significantly different. A Pearson's correlation test was then used to examine the relationship between the latency of the beat-related SS-EP and the hand tapping movement, the movement-related SS-EP and the hand tapping movement, as well as the beat-related and movement-related SS-EPs.

Topographical Distribution of the SS-EPs

Current source density (CSD) estimates of the band-pass filtered time-domain EEG signals averaged relative to beat onset were used to better assess the differences between the topographical distributions of the 2.4-Hz beat-related SS-EPs, the 1.2-Hz movement-related SS-EPs, and the 3.6-Hz cross-modulation SS-EPs obtained in each condition (Fig. 6). Topographical maps were computed using the group-level average signals, after normalization of the values of each subject. The estimates were computed using spherical spline interpolation, as implemented in the CSD toolbox (Kayser and Tenke 2006). For each frequency and condition, group-level average topographical maps were computed at the latency of maximum global field power. We then examined in these CSD estimates whether the topographical distributions of the 1.2-Hz movement-related SS-EP was lateralized relative to the tapping hand (Fig. 6). For each subject and hand tapping condition, the magnitude of the 1.2-Hz SS-EP recorded at the central electrode ipsilateral to the tapping hand (C4 and C3, for right and left hand tapping, respectively) was compared with the magnitude recorded at the central electrode contralateral to the tapping hand (electrodes C3 and C4, for right and left hand tapping, respectively), using a paired-sample *t*-test (Coles 1989). The same procedure was used to assess the lateralization of the 2.4-Hz beat-related SS-EP as well as the 3.6-Hz SS-EP, using electrodes FC2 and FC1, as these electrodes showed the highest magnitude in the group-level averaged maps (Fig. 6).

Finally, a Pearson's correlation test was then used to assess the relationship between the topographical distributions of the 1.2- and 2.4-Hz SS-EPs, the 1.2- and 3.6-Hz SS-EPs, as well as the 2.4- and 3.6-Hz SS-EPs.

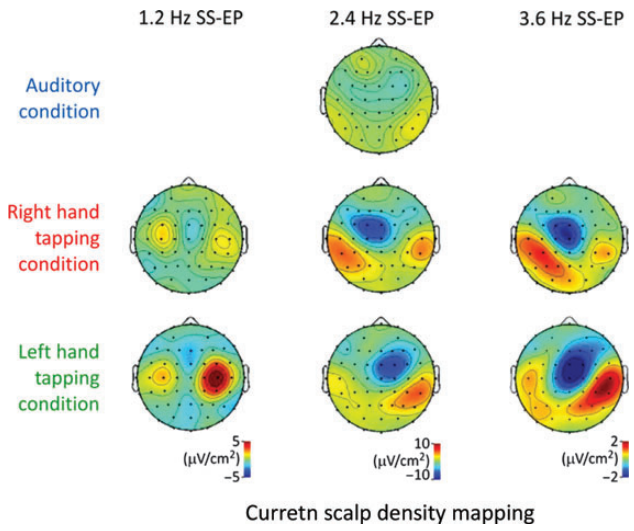

Figure 6. Topographic maps (group-level average current scalp density) of the 1.2-, 2.4-, and 3.6-Hz SS-EPs obtained in the control auditory condition, the right hand tapping condition and the left hand tapping condition.

Dipolar Source Analysis of the SS-EPs

We also performed a dipolar source analysis to examine whether the sources explaining the 2.4-Hz SS-EP obtained in the auditory condition, the sources explaining the 1.2-Hz SS-EP obtained in the right and left hand tapping conditions, or the combination of these 2 models could explain the topographical distribution of the 2.4- and 3.6-Hz SS-EPs obtained in the left and right hand tapping conditions. The analyses were performed on the group-level average scalp topographies of the 1.2-, 2.4-, and 3.6-Hz SS-EPs, using *dipfit2*, an algorithm based on a nonlinear optimization technique and a standardized boundary head element model (Oostendorp and van Oosterom 1989), as implemented in the Fieldtrip toolbox (Oostenveld et al. 2011).

Results

Hand Tapping Movement

The noise-subtracted frequency amplitude spectra of the accelerometer signals was, at 1.2 Hz, significantly greater than zero in both the right ($t = 4.21$, $P = 0.004$, $df = 7$) and the left ($t = 4.58$, $P = 0.002$, $df = 7$) hand tapping conditions (Fig. 1). The magnitude of the 1.2-Hz hand movement signal was not significantly different across the 2 tapping conditions ($t = 0.33$, $P = 0.74$, $df = 7$) (Fig. 1).

EEG Frequency Spectra

As shown at the group-level average of the frequency spectra (Fig. 2) as well as the individual-level frequency spectra (Fig. 3), in all 3 conditions, the auditory beat elicited a clear increase of signal amplitude at 2.4 Hz, corresponding to the frequency of the beat, and referred to as beat-related SS-EP. The term "beat" was used because the frequency of the periodic modulation of the auditory stimulus was within the frequency range of musical tempo, that is, a frequency at which sensorimotor synchronization to periodic sensory input is frequently observed. Hence, the neural activity captured in this SS-EP could, at least in part, be functionally distinct from that captured by auditory SS-EPs elicited using higher stimulation frequencies (e.g., 20–40 Hz; Draganova et al. 2002). In the left and right hand tapping conditions, an additional peak in the EEG frequency spectra was observed at 1.2 Hz, corresponding to the frequency of the tapping movement, and referred to as movement-related SS-EP. In these conditions, a third peak was also observed at 3.6 Hz, referred to as cross-modulation SS-EP.

Beat-Related 2.4 Hz SS-EP

The noise-subtracted amplitude of the 2.4-Hz beat-related SS-EP, averaged across all scalp electrodes, was 0.09 ± 0.01 μV

in the control auditory condition, 0.33 ± 0.03 μV in the right hand tapping condition, and 0.34 ± 0.05 μV in the left hand tapping condition (mean ± standard error of the mean) (Figs 2 and 3). The increase in signal amplitude at this frequency was significant in all 3 conditions (control auditory condition: $t = 6.05$, $P = 0.0005$, df = 7; right hand tapping condition: $t = 10.1$, $P < 0.0001$, df = 7; left hand tapping condition: $t = 6.6$, $P = 0.0003$, df = 7). The magnitude of the beat-related SS-EP was significantly different across conditions ($F = 31.7$, $P < 0.0001$, $\eta^2 = 0.82$, df = 7) (Figs 2 and 3). Post hoc comparisons showed that the magnitude of the EEG signal at 2.4 Hz was significantly greater in both hand tapping conditions when compared with the control auditory condition (right hand tapping condition: $t = 9.6$, $P < 0.0001$, df = 7; left hand tapping condition: $t = 5.3$, $P = 0.001$, df = 7) (Figs 2 and 3). As shown in Figure 6, in the control auditory condition, the scalp topography of the beat-related SS-EP was maximal over frontal and temporal regions, and symmetrically distributed over both hemispheres. In contrast, in the left and right hand tapping conditions, the scalp topographies were clearly asymmetrical, and maximal over the hemisphere contralateral to the tapping hand. Comparison of the signals recorded at electrodes FC1 and FC2 confirmed this lateralization of the beat-related SS-EP in the hand tapping conditions ($t = 5.38$, $P = 0.001$, df = 7).

Movement-Related 1.2 Hz SS-EP

The noise-subtracted amplitude of the 1.2-Hz movement-related SS-EP, averaged across all scalp electrodes, was 0.005 ± 0.006 μV in the control auditory condition, 0.08 ± 0.01 μV in the right hand tapping condition, and 0.12 ± 0.01 μV in the left hand tapping condition (Figs 2 and 3). The increase of signal amplitude at this frequency was significant in the right and left hand tapping conditions (right hand tapping condition: $t = 6.3$, $P = 0.0004$, df = 7; left hand tapping condition: $t = 8.9$, $P < 0.0001$, df = 7), but not in the control auditory condition ($t = 0.89$, $P = 0.4$, df = 7). The magnitude of the movement-related SS-EP was significantly different across conditions ($F = 19.1$, $P < 0.0001$, $\eta^2 = 0.73$, df = 7) (Figs 2 and 3). Post hoc comparisons showed that the magnitude of the EEG signal at 1.2 Hz was significantly greater in the right and left hand tapping conditions than in the control auditory condition (left hand tapping condition: $t = 4.8$, $P = 0.002$, df = 7; right hand tapping condition: $t = 8.4$, $P < 0.0001$, df = 7) (Figs 2 and 3). As shown in Figures 2 and 6, the scalp topography of the movement-related SS-EP was maximal over the central region contralateral to the hand movement. Comparison of the signals recorded at electrodes C3 and C4 confirmed a significant lateralization of the movement-related SS-EP ($t = 3.32$, $P = 0.01$, df = 7).

Cross-Modulation 3.6 Hz SS-EP

The noise-subtracted amplitude of the 3.6-Hz cross-modulation SS-EP, averaged across all scalp electrodes, was -0.001 ± 0.003 μV in the control auditory condition, 0.035 ± 0.01 μV in the right hand tapping condition and 0.05 ± 0.02 μV in the left hand tapping condition (Figs 2 and 3). The increase in signal amplitude at this frequency was significant in the right and left hand tapping conditions (right hand tapping condition: $t = 3.53$, $P = 0.01$, df = 7; left hand tapping condition: $t = 3.86$, $P = 0.006$, df = 7), but not in the control auditory condition ($t = 0.36$, $P = 0.73$, df = 7). The magnitude of this additional SS-EP was significantly different across conditions ($F = 10.5$, $P = 0.001$, $\eta^2 = 0.6$, df = 7) (Figs 2 and 3). Post hoc comparisons showed that the magnitude of the EEG signal at 3.6 Hz was significantly greater in the right and left hand tapping conditions than in the control auditory condition (right hand tapping condition: $t = 3.4$, $P = 0.012$, df = 7; left hand tapping condition: $t = 3.8$, $P = 0.007$, df = 7) (Fig. 3). As shown in Figure 6, the scalp topography of the 3.6-Hz SS-EP observed in the left and right hand tapping conditions was very similar to that of the 2.4-Hz SS-EP obtained in these same conditions. Both displayed a maximum over frontal and temporal regions, were clearly asymmetrical, and maximal over the hemisphere contralateral to the tapping hand. Comparison of the signals recorded at electrodes FC1 and FC2 confirmed the lateralization of the 3.6-Hz SS-EP obtained in the left and right hand tapping conditions ($t = 3.21$, $P = 0.01$, df = 7).

Phase Coupling Between Movement, Movement-Related SS-EPs and Beat-Related SS-EPs

The mean latency of the tapping movement was −0.036 ± 0.01 s in the right hand tapping condition and −0.046 ± 0.01 s in the left hand tapping condition, relative to the actual occurrence of the beat (Fig. 5). These latencies were significantly different from zero (right hand tapping condition: $t = 32.5$, $P < 0.0001$, df = 7; left hand tapping condition: $t = 39.69$, $P < 0.0001$, df = 7). That is, subjects exhibited a mean negative asynchrony in their synchronization performance (Repp 2005; Aschersleben 2002), that is, a systematic anticipation of the hand tapping movement relative to the beat onset, ranging from a hundred of ms before the beat for some subjects to no anticipation for other subjects (Fig. 5). The tapping latencies were not significantly different across the 2 tapping conditions ($t = 1.17$, $P = 0.28$, df = 7) (Fig. 5).

The latency of the beat-related SS-EP, expressed relative to the actual beat occurrence, was 0.044 ± 0.02 s in the control auditory condition, 0.154 ± 0.01 s in the right hand tapping condition and 0.144 ± 0.01 s in the left hand tapping condition. These values were significantly different across conditions ($F = 12.37$, $P = 0.0008$, $\eta^2 = 0.63$, df = 7). Post hoc comparisons showed that the relative latency of the beat-related SS-EP obtained in the control auditory condition was significantly different from the relative latency of the beat-related SS-EP obtained in both the right hand tapping condition ($t = 3.63$, $P = 0.008$, df = 7) as well as the left hand tapping condition ($t = 3.39$, $P = 0.01$, df = 7).

The relative latency of the movement-related SS-EP was of −0.336 ± 0.2 s in the right hand tapping condition and −0.306 ± 0.02 s in the left hand tapping condition. These values were not significantly different across the 2 tapping conditions ($t = 1.77$, $P = 0.12$, df = 7).

There was a significant correlation between the relative latencies of the beat-related SS-EP and the hand tapping movement ($r^2 = 0.53$, $P = 0.03$) (Fig. 5). There was also a significant correlation between the relative latencies of the movement-related SS-EP and the hand tapping movement ($r^2 = 0.48$, $P = 0.05$), and between the relative latencies of the movement- and beat-related SS-EPs ($r^2 = 0.66$, $P = 0.01$).

Relationship Between the Topographical Distributions of Beat-Related, Movement-Related and Cross-Modulation SS-EPs

A significant correlation was found between the scalp topographies of the 3.6-Hz cross-modulation SS-EP and the 2.4-Hz

beat-related SS-EP (right hand tapping: $r^2 = 0.69$, $P < 0.0001$; left hand tapping: $r^2 = 0.64$, $P < 0.0001$). In contrast, there was no significant correlation between the scalp topographies of the 3.6-Hz SS-EP and the 1.2-Hz movement-related SS-EP (right hand tapping: $r^2 = 0.04$, $P = 0.11$; left hand tapping: $r^2 = 0.005$, $P = 0.53$). Furthermore, there was also no significant correlation between the 1.2-Hz and the 2.4-Hz SS-EPs in the left hand tapping condition ($r^2 = 0.01$, $P = 0.29$), and a weak negative correlation in the right hand tapping condition ($r^2 = 0.017$, $P = 0.001$).

Dipolar Modeling of Beat-Related, Movement-Related and Cross-Modulation SS-EPs

To examine whether the sources explaining the 2.4-Hz beat-related SS-EP obtained in the auditory condition, or the sources explaining the 1.2-Hz movement-related SS-EPs could explain the 2.4- and 3.6-Hz SS-EPs obtained in the right and left hand tapping conditions, we performed the following dipolar source analysis on the group-level average scalp topographies.

First, to obtain a dipolar model of the sources contributing to the activity related to the auditory beat, we fitted a symmetrical pair of dipoles (symmetrical location in the left and right hemisphere; unconstrained dipole orientations and magnitudes) to the scalp topography of the 2.4-Hz SS-EP obtained in the auditory condition (Fig. 7). The residual variance of the obtained fit was 2%. Second, to obtain a dipolar model of the sources contributing to the activity related to the hand tapping movement, we fitted a single dipole as well as a symmetrical pair of dipoles to the scalp topographies of the 1.2-Hz SS-EPs obtained in the right and left hand tapping conditions. The residual variance of the single dipole model was 21% (right hand tapping condition) and 13% (left hand tapping condition). The higher residual variance obtained in the right hand tapping condition could be due to the lower signal-to-noise ratio of the 1.2-Hz SS-EP obtained in that condition. Nevertheless, in both the right and the left hand tapping conditions, the location of the dipoles was compatible with activity originating from sensorimotor areas contralateral to the tapping hand. When compared with the residual variance of the single dipole model, the residual variance of the symmetrical dipoles model was not markedly improved (right hand tapping condition: 18%, left hand tapping condition: 8%). Furthermore, in the right hand tapping condition, the solution was not physiologically meaningful (2 dipoles located at the midline, pointing in opposite directions).

Then, we compared how each of these different dipole models, as well as the combination of these dipole models could explain the scalp topographies of the 2.4- and 3.6-SS-EPs obtained in the right and left hand tapping conditions. Because our aim was to examine whether these SS-EPs could be explained by activity originating from the cortical structures generating the 2.4-Hz SS-EP in the auditory condition and/or the 1.2-HZ SS-EP in the right and left hand tapping conditions, the location and orientation of the dipoles was fixed, and only the magnitude of the dipoles was adjusted.

In both the right and the left hand tapping conditions, we found that the residual variance of the fit obtained when adjusting the dipole model of the 2.4-Hz beat-related SS-EP of the auditory condition to the scalp topographies of the 2.4- and 3.6-Hz SS-EPs of the hand tapping conditions was markedly lower than the residual variance of the fit obtained when adjusting the dipole models of the 1.2-Hz movement-related SS-EPs (Table 1). Moreover, we found that fitting the dipole models of the 1.2-Hz movement-related SS-EPs to the residual scalp topographies of the 2.4- and 3.6-Hz SS-EPs obtained from fitting the dipole model explaining the 2.4-Hz beat-related SS-EP of the auditory condition did not improve the residual variance. This suggests that the 2.4- and 3.6-Hz SS-EPs of the hand tapping conditions could receive a strong contribution from the cortical sources generating the 2.4-Hz SS-EP obtained in the auditory condition, but not the cortical sources generating the 1.2-Hz SS-EPs obtained in the hand tapping conditions.

Interestingly, in both 2.4- and 3.6-Hz SS-EPs of the right and the left hand tapping conditions, the magnitude of the dipole located in the hemisphere contralateral to the tapping hand was greater than the magnitude of the dipole located in the ipsilateral hemisphere (Table 2).

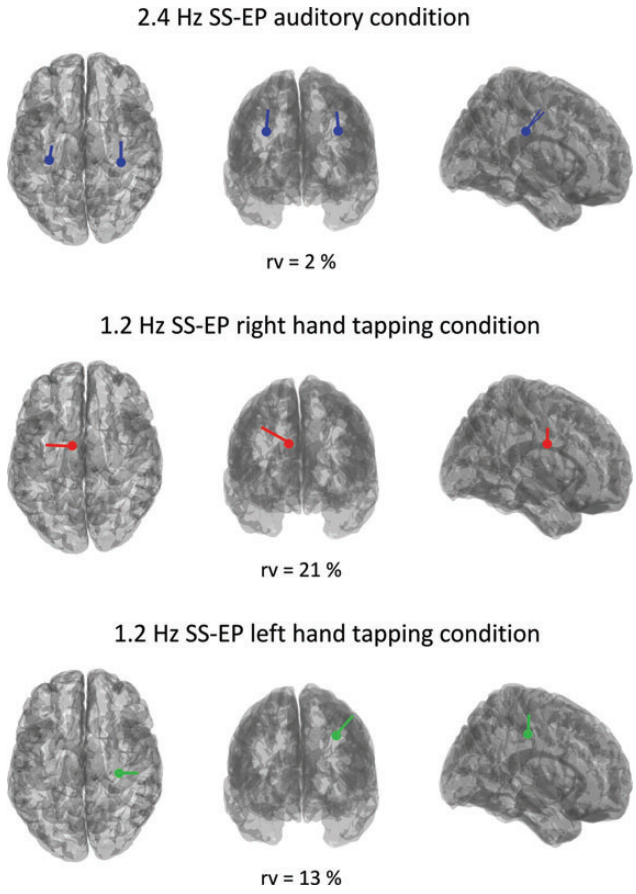

Figure 7. Source analysis. The scalp topography of the 2.4-Hz beat-related SS-EP obtained in the auditory condition was modeled using a symmetric pair of dipoles (dipoles shown in blue). The scalp topographies of the 1.2-Hz movement-related SS-EPs obtained in the right and left hand tapping conditions were modeled using a single dipole (dipoles shown in red and green, respectively).

Discussion

The objective of the present study was to explore how distant brain areas supporting cooperative perception and action coordinate their dynamics during rhythmic sensorimotor synchronization. We found that moving to the beat is associated with

Table 1
Residual variances obtained when adjusting the magnitudes of the dipole models explaining the 2.4-Hz SS-EPs in the auditory condition, the 1.2-Hz SS-EPs in the left and right hand tapping conditions, and a combination of this 2 models onto the 2.4- and 3.6-Hz SS-EPs obtained in the left and right hand tapping conditions

	Dipole model explaining the 2.4-Hz SS-EP in the auditory condition	Dipole models explaining the 1.2-Hz SS-EPs in the hand tapping conditions		Combination of the dipole pair explaining the 2.4-Hz SS-EP in the auditory condition and the single dipole explaining the 1.2-Hz SS-EP in the hand tapping conditions
	Dipole pair (%)	Single dipole (%)	Dipole pair (%)	Three dipoles (%)
2.4-Hz SS-EP				
Right hand condition	15	26	23	15
Left hand condition	12	24	22	12
3.6-Hz SS-EP				
Right hand condition	14	41	39	14
Left hand condition	29	34	29	29

Table 2
Magnitude of the dipoles obtained by fitting the model explaining the 2.4-Hz SS-EP in the auditory condition onto the 2.4- and 3.6-Hz SS-EPs obtained in the left and right hand tapping conditions

	Dipole magnitudes (nAm)	
	Left hemisphere	Right hemisphere
2.4-Hz SS-EP		
Right hand tapping condition	0.0120	0.0106
Left hand tapping condition	0.0075	0.0178
3.6-Hz SS-EP		
Right hand tapping condition	0.0084	0.0080
Left hand tapping condition	0.0054	0.0124

the emergence of periodic neural activities which can be captured in the human EEG as SS-EPs. Indeed, when subjects tapped to the beat, the EEG was characterized by 1) a 2.4-Hz SS-EP compatible with beat-related entrainment whose scalp topography could be explained by sources located in auditory areas, 2) a 1.2-Hz SS-EP compatible with movement-related entrainment whose scalp topography could be explained by sources located in motor and/or somatosensory areas contralateral to the tapping hand, and 3) a 3.6-Hz SS-EP whose frequency, corresponding to the sum of beat and movement frequencies, suggests a nonlinear cross-modulation product of sensorimotor integration, that is, the activity of neurons onto which auditory- and movement-related activities converge (Ding and Simon 2009; Wang et al. 2012; Giani et al. 2012). Furthermore, we observed 4) a tight phase coupling of beat- and movement-related SS-EPs, and 5) a selective enhancement of beat- and cross-modulation SS-EPs over the hemisphere contralateral to the tapping hand, suggesting that the activity related to the rhythmic movement may exert a top-down effect on the processing of the auditory beat.

Beat- and Movement-Related SS-EPs

Cortical responses were elicited in the present study by the long-lasting periodic repetition of an auditory beat and by the long-lasting periodic production of a hand tapping movement at half the frequency of the auditory beat. These responses were observed in the EEG spectrum in the form of a beat- and movement-related SS-EP appearing at the exact frequency of the beat and movement (Regan 1989; Nozaradan et al. 2011). Whether these activities result from the stimulus-driven entrainment of a network of neurons responding to this periodicity, or whether they reflect the linear summation of successive transient ERPs elicited by the onset of each periodic event remains an open question, and the 2 hypotheses may coexist (Galambos et al. 1981; Draganova et al. 2002).

In the control auditory condition, the topography of the beat-related SS-EP was maximal over frontal and temporal electrodes and symmetrically distributed over the 2 hemispheres (Fig. 6). This topographical distribution, such as the results of the dipole fitting procedure (Fig. 7) was similar to that of mid- and late-latency auditory ERPs (Galambos et al. 1981; Draganova et al. 2002; Wang et al. 2012) as well as that of auditory SS-EPs elicited by higher stimulation frequencies (e.g., 20–40 Hz; Johnson et al. 1988). Hence, it seems likely that the bulk of the beat-related SS-EP, such as auditory ERPs and SS-EPs, mainly reflects activity originating bilaterally from auditory cortices.

In the hand tapping conditions, the rhythmic movements elicited a periodic signal in the EEG which was observed in the EEG spectrum at the frequency corresponding to the frequency of the periodic movement. The scalp topography of this response was maximal over the central region contralateral to the moving hand (Figs 2 and 6). This supports the view that the production of periodic movements is related to the periodic activity of neurons located within the hand representation of the contralateral primary motor and/or somatosensory cortex (Gerloff et al. 1997, 1998; Kopp et al. 2000; Daffertshofer et al. 2005; Kourtis et al. 2008; Bourguignon et al. 2011). However, as for the beat-related SS-EP, whether these activities result from the stimulus-driven entrainment of neurons, or whether they reflect the linear summation of successive transient ERPs elicited by the periodic repetition of the movement remains an open question.

Sensorimotor Integration: Evidence and Alternative Interpretations

Cross-Modulation SS-EP

In addition to the 2.4-Hz beat-related SS-EP and the 1.2-Hz movement-related SS-EP, moving to the beat elicited a third SS-EP appearing at 3.6 Hz. Such a response cannot be explained by the simple linear summation of the 1.2- and 2.4-Hz oscillatory activities in the time domain, as this would not have resulted in activity at 3.6 Hz (Regan 1989; Giani et al. 2012). Hence, this 3.6-Hz activity is likely to reflect a nonlinear cross-modulation product of beat- and movement-related oscillations. Indeed, when 2 distinct neural populations oscillate at 2 distinct frequencies, cross-modulation frequencies, corresponding to the sum or difference of the 2 main frequencies, may emerge if the signals conveyed by each of the 2 oscillating populations converge onto another population integrating these inputs (Zemon and Ratliff 1984; Regan 1989; Regan et al. 1995; Williams et al. 2004; Appelbaum et al. 2008; Sutoyo and

Srinivasan 2009). Using scalp EEG recordings, nonlinear cross-modulation SS-EPs have already been reported within visual (Zemon and Ratliff 1984; Regan 1989; Regan et al. 1995; Appelbaum et al. 2008; Sutoyo and Srinivasan 2009) and auditory (Purcell et al. 2007; Wile and Balaban 2007) sensory modalities; and the existence of neurons producing such responses has been confirmed using single-cell recordings (Williams et al. 2004). Hence, the finding that moving to the beat is not only related to the presence of beat- and movement-related SS-EPs but also leads to the emergence of a cross-modulation SS-EP appearing at 3.6 Hz, that is, at the sum of the 2.4-Hz beat-related neural entrainment and the 1.2-Hz movement-related neural entrainment frequencies, could indicate the existence of a nonlinear process of convergence of sensory- and motor-related periodic activities, possibly reflecting the activity of a population of neurons whose output corresponds to the product of the 2 input oscillations (Ding and Simon 2009; Wang et al. 2012; Giani et al. 2012).

Previous studies have already reported evidence for sensorimotor interactions, in the form of a modulation of transient ERPs (Lütkenhöner et al. 2002; Praamstra et al. 2003), as well as a modulation of oscillatory patterns of neural activity within the gamma (30 Hz and more) or beta frequency range (between 15 and 30 Hz) (see, e.g., Roelfsema et al. 1997 or Donoghue et al. 1998). Importantly, our finding is compatible with these observations, and do not contradict the hypothesis that synchronization between distant cortical areas is supported by fast oscillatory activity that is not imposed by the periodicity of the stimulus.

Phase Coupling of Beat- and Movement-Related SS-EPs

On average, the hand tapping movement preceded the actual occurrence of the beat. This anticipation of the hand tapping movement is a well-described phenomenon, referred to as mean negative asynchrony (Aschersleben 2002; Repp 2005). Such as in other studies (Aschersleben 2002; Repp 2005), the negative asynchrony was reproducible within subjects and across the 2 hands, but varied greatly between subjects, from no anticipation to more than 100 ms (Fig. 5). The latency of the hand tapping movement was strongly correlated with the latency of the movement-related SS-EP, supporting the view that the production of rhythmic movements is related to neural activity time-locked to the produced movement and/or the somatosensory feedback (Gerloff et al. 1997, 1998; Kopp et al. 2000; Daffertshofer et al. 2005; Kourtis et al. 2008; Bourguignon et al. 2011).

More surprising was the finding of a significant correlation between the latency of the hand tapping movement and the latency of the beat-related SS-EP (Fig. 5). Although a contamination of movement-related activities at 2.4 Hz cannot be entirely excluded, this observation suggests that the timing of the neural entrainment to the beat was not only dependent on the timing of the eliciting auditory beat, but was also modulated according to the timing of the produced synchronized movement. This observation suggests that the production of synchronized hand movements may modulate the neural representation of the auditory beat, possibly contributing to an accurate sensorimotor synchronization. Furthermore, it suggests that the amount of movement asynchrony is already encoded at an early sensory level, that is, within the neural representation of the beat.

To summarize, our finding suggests that during rhythmic sensorimotor synchronization, coupling occurs between the distant brain areas supporting beat- and movement-related neural entrainment.

Movement-Induced Enhancement of the Beat-Related SS-EP

The magnitude of the 2.4-Hz beat-related SS-EP was significantly enhanced in the hand tapping conditions when compared with the control auditory condition. This enhancement was much more pronounced over the hemisphere contralateral to the moving hand (Fig. 6). Source analysis using dipole modeling showed that the cortical sources explaining the 2.4-Hz SS-EP obtained in the auditory condition—but not the cortical sources explaining the 1.2-Hz movement-related SS-EP obtained in the hand tapping conditions—could satisfactorily explain the scalp topography of the 2.4-Hz SS-EPs obtained in the left and right hand tapping conditions (Fig. 7). Therefore, we hypothesize that the lateralized enhancement of the 2.4-Hz SS-EP observed in the left and right hand tapping conditions resulted from movement exerting a top down effect on the processing of the auditory beat, in particular, within the hemisphere involved in producing the movement. However, because of the low spatial resolution of EEG data and the inherent uncertainty of EEG source analysis, interpretation of these findings has to be taken cautiously. Future studies based on other methods to sample brain activity such as magnetoencephalography, functional magnetic resonance imaging or the invasive recording of local field potentials are needed to confirm this interpretation. Indeed, because of its complex signature, one cannot exclude that movement-related processes generate activity at harmonic frequencies within neuronal populations that are different from the neuronal populations responsible for the 1.2-Hz SS-EP. Hence, the lateralized enhancement of the 2.4-Hz SS-EP could also be explained by a contribution of movement-related activity distinct from the activity underlying the 1.2-Hz SS-EP.

Conclusion

Taken together, the results of the present study suggest that rhythmic sensorimotor synchronization involves a dynamic coupling and interaction of sensory- and movement-related neuronal entrainments. More generally, our findings suggest that the recording of SS-EPs constitutes a promising approach to gain insight on the dynamics of neural activity underlying cooperative perception and action.

Supplementary Material

Supplementary material can be found at: http://www.cercor.oxfordjournals.org/

Funding

S.N. is supported by the Fund for Scientific Research of the French-speaking community of Belgium (F.R.S.-FNRS). A.M. has received the support from the French-speaking community of Belgium (F.R.S.-FNRS) FRSM 3.4558.12 Convention Grant. I.P. is supported by the Natural Sciences and Engineering Research Council of Canada, the Canadian Institutes of Health Research and by a Canada Research Chair.

Notes

Conflict of Interest: None declared.

References

Appelbaum LG, Wade AR, Pettet MW, Vildavski VY, Norcia AM. 2008. Figure-ground interaction in the human visual cortex. J Vis. 8:8.1–819.

Aschersleben G. 2002. Temporal control of movements in sensorimotor synchronization. Brain Cogn. 48(1):66–79.

Bach M, Meigen T. 1999. Do's and don'ts in Fourier analysis of steady-state potentials. Doc Ophthalmol. 99:69–82.

Beek PJ, Peper CE, Daffertshofer A. 2002. Modeling rhythmic interlimb coordination: beyond the Haken-Kelso-Bunz model. Brain Cogn. 48:149–165.

Bell AJ, Sejnowski TJ. 1995. An information-maximization approach to blind separation and blind deconvolution. Neural Comput. 7:1129–1159.

Bourguignon M, De Tiège X, Op de Beeck M, Pirotte B, Van Bogaert P, Goldman S, Hari R, Jousmäki V. 2011. Functional motor-cortex mapping using corticokinematic coherence. Neuroimage. 55:1475–1479.

Brainard DH. 1997. The psychophysics toolbox. Spat Vis. 10:433–436.

Chen JL, Penhune VB, Zatorre RJ. 2008. Listening to musical rhythms recruits motor regions of the brain. Cereb Cortex. 18:2844–2854.

Coles MG. 1989. Modern mind-brain reading: psychophysiology, physiology, and cognition. Psychophysiology. 26:251–269.

Colon E, Nozaradan S, Legrain V, Mouraux A. 2012. Steady-state evoked potentials to tag specific components of nociceptive cortical processing. Neuroimage. 60(1):571–581.

Daffertshofer A, Peper CL, Beek PJ. 2005. Stabilization of bimanual coordination due to active interhemispheric inhibition: a dynamical account. BiolCybern. 92:101–109. .

Ding N, Simon JZ. 2009. Neural representations of complex temporal modulations in the human auditory cortex. J Neurophysiol. 102 (5):2731–2743.

Donoghue JP, Sanes JN, Hatsopoulos NG, Gaál G. 1998. Neural discharge and local field potential oscillations in primate motor cortex during voluntary movements. J Neurophysiol. 79(1):159–173.

Draganova R, Ross B, Borgmann C, Pantev C. 2002. Auditory cortical response patterns to multiple rhythms of AM sound. Ear Hear. 23:254–265.

Drake C, Botte MC. 1993. Tempo sensitivity in auditory sequences: evidence for a multiple look model. Percept Psychophys. 54:277–286.

Frigo M, Johnson SG. 1998. FFTW: an adaptive software architecture for the FFT. Proceedings of the 1998 IEEE International Conference on Acoustics, Speech and Signal Processing. Vol. 3:1381–1384.

Galambos R, Makeig S, Talmachoff PJ. 1981. A 40-Hz auditory potential recorded from the human scalp. Proc Natl Acad Sci USA. 78:2643–2647.

Gerloff C, Toro C, Uenishi N, Cohen LG, Leocani L, Hallett M. 1997. Steady-state movement-related cortical potentials: a new approach to assessing cortical activity associated with fast repetitive finger movements. Electroencephalogr Clin Neurophysiol. 102:106–113.

Gerloff C, Uenishi N, Nagamine T, Kunieda T, Hallett M, Shibasaki H. 1998. Cortical activation during fast repetitive finger movements in humans: steady-state movement-related magnetic fields and their cortical generators. Electroencephalogr Clin Neurophysiol. 109:444–453.

Giani AS, Ortiz E, Belardinelli P, Kleiner M, Preissl H, Noppeney U. 2012. Steady-state responses in MEG demonstrate information integration within but not across the auditory and visual senses. Neuroimage. 60:1478–1489.

Grahn JA, Brett M. 2007. Rhythm and beat perception in motor areas of the brain. J Cogn Neurosci. 19:893–906.

Hogan N, Sternad D. 2007. On rhythmic and discrete movements: reflections, definitions and implications for motor control. Exp Brain Res. 181:13–30.

Janata P, Tomic ST, Haberman JM. 2012. Sensorimotor coupling in music and the psychology of the groove. J Exp Psychol Gen. 141 (1):54–75.

Johnson BW, Weinberg H, Ribary U, Cheyne DO, Ancill R. 1988. Topographic distribution of the 40 Hz auditory evoked-related potential in normal and aged subjects. Brain Topogr. 1(2):117–121.

Jones MR, Boltz M. 1989. Dynamic attending and responses to time. Psychol Rev. 96:459–491.

Jung TP, Makeig S, Westerfield M, Townsend J, Courchesne E, Sejnowski TJ. 2000. Removal of eye activity artifacts from visual event-related potentials in normal and clinical subjects. Clin Neurophysiol. 111:1745–1758.

Kayser J, Tenke CE. 2006. Principal components analysis of Laplacian waveforms as a generic method for identifying ERP generator patterns: I. evaluation with auditory oddball tasks. Clin Neurophysiol. 117(2):348–368.

Kopp B, Kunkel A, Müller G, Mühlnickel W, Flor H. 2000. Steady-state movement-related potentials evoked by fast repetitive movements. Brain Topogr. 13:21–28.

Kourtis D, Seiss E, Praamstra P. 2008. Movement-related changes in cortical excitability: a steady-state SEP approach. Brain Res. 1244:113–120.

Large EW. 2008. Resonating to musical rhythm: theory and experiment. In Grondin Simon, editors. The psychology of time. West Yorkshire: Emerald.

Large EW, Jones MR. 1999. The dynamics of attending: how we track time varying events. Psychol Rev. 106:119–159.

Large EW, Kolen JF. 1994. Resonance and the perception of musical meter. Connect Sci. 6:177–208.

London J. 2004. Hearing in time: psychological aspects of musical meter. Oxford University Press Inc.

Lütkenhöner B, Lammertmann C, Simões C, Hari R. 2002. Magnetoencephalographic correlates of audiotactile interaction. Neuroimage. 15:509–522.

Madison G. 2006. Experiencing groove induced by music: consistency and phenomenology. Music Percept. 24:201–208.

Makeig S. 2002. Response: event-related brain dynamics - unifying brain electrophysiology. Trends Neurosci. 25:390.

Mouraux A, Iannetti GD. 2008. Across-trial averaging of event-related EEG responses and beyond. Magn Reson Imaging. 26:1041–1054.

Mouraux A, Iannetti GD, Colon E, Nozaradan S, Legrain V, Plaghki L. 2011. Nociceptive steady-state evoked potentials elicited by rapid periodic thermal stimulation of cutaneous nociceptors. J Neurosci. 31:6079–6087.

Nozaradan S, Peretz I, Missal M, Mouraux A. 2011. Tagging the neuronal entrainment to beat and meter. J Neurosci. 31:10234–10240.

Nozaradan S, Peretz I, Mouraux A. 2012a. Selective neuronal entrainment to the beat and meter embedded in a musical rhythm. J Neurosci. 32:17572–17581.

Nozaradan S, Peretz I, Mouraux A. 2012b. Steady-state evoked potentials as an index of multisensory temporal binding. NeuroImage. 60:21–28.

Oostendorp TF, van Oosterom A. 1989. Source parameter estimation in inhomogeneous volume conductors of arbitrary shape. IEEE Trans Biomed Eng. 36(3):382–391.

Oostenveld R, Fries P, Maris E, Schoffelen JM. 2011. Field Trip: Open source software for advanced analysis of MEG, EEG, and invasive electrophysiological data. Comput Intell Neurosci. 2011:156869.

Phillips-Silver J, Aktipis CA, Bryant GA. 2010. The ecology of entrainment: foundations of coordinated rhythmic movement. Music Percept. 28:3–14.

Phillips-Silver J, Trainor LJ. 2005. Feeling the beat: movement influences infant rhythm perception. Science. 308:1430.

Phillips-Silver J, Trainor LJ. 2007. Hearing what the body feels: auditory encoding of rhythmic movement. Cognition. 105:533–546.

Pollok B, Müller K, Aschersleben G, Schnitzler A, Prinz W. 2004. The role of the primary somatosensory cortex in an auditorily paced finger tapping task. Exp Brain Res. 156:111–117.

Praamstra P, Turgeon M, Hesse CW, Wing AM, Perryer L. 2003. Neurophysiological correlates of error correction in sensorimotor-synchronization. Neuroimage. 20:1283–1297.

Pressing J. 1998. Error correction processes in temporal pattern production. J Math Psychol. 42:63–101.

Purcell DW, Ross B, Picton TW, Pantev C. 2007. Cortical responses to the $2f_1$-f_2 combination tone measured indirectly using magnetoencephalography. J Acoust Soc Am. 122:992–1003.

Regan D. 1989. Human brain electrophysiology: evoked potentials and evoked magnetic fields in science and medicine. New York: Elsevier.

Regan MP, He P, Regan D. 1995. An Audiovisual Convergence Area in Human Brain. Exp Brain Res. 106:485–487.
Repp BH. 2005. Sensorimotor synchronization: a review of the tapping literature. Psychon B Rev. 12:969–992.
Roelfsema PR, Engel AK, König P, Singer W. 1997. Visuomotor integration is associated with zero time-lag synchronization among cortical areas. Nature. 385(6612):157–161.
Saupe K, Schröger E, Andersen SK, Müller MM. 2009. Neural mechanisms of intermodal sustained selective attention with concurrently presented auditory and visual stimuli. Front Hum Neurosci. 3:58.
Sutoyo D, Srinivasan R. 2009. Nonlinear SSVEP responses are sensitive to the perceptual binding of visual hemifields during conventional 'eye' rivalry and interocular 'percept' rivalry. Brain Res. 28:1251245–1251255.
Teki S, Grube M, Kumar S, Griffiths TD. 2011. Distinct neural substrates of duration-based and beat-based auditory timing. J Neurosci. 31:3805–3812.
vanNoorden L, Moelants D. 1999. Resonance in the perception of musical pulse. J New Music Res. 28:43–66.
Vorberg D, Wing AM. 1995. Modeling variability and dependence in timing. In Heuer H, Keele SW, editors. Handbook of perception and action. London: Academic Press.
Wang Y, Ding N, Ahmar N, Xiang J, Poeppel D, Simon JZ. 2012. Sensitivity to temporal modulation rate and spectral bandwidth in the human auditory system: MEG evidence. J Neurophysiol. 107 (8):2033–2041.
Wile D, Balaban E. 2007. An auditory neural correlate suggests a mechanism underlying holistic pitch perception. PLoS ONE. 2(4):e369.
Williams PE, Mechler F, Gordon J, Shapley R, Hawken MJ. 2004. Entrainment to video displays in primary visual cortex of macaque and humans. J Neurosci. 24:8278–8288.
Zemon V, Ratliff F. 1984. Intermodulation components of the visual evoked potential: responses to lateral and superimposed stimuli. Biol Cybern. 50:401–408.